A DENOISING METHOD FOR WHOLE-BODY LOW-DOSE X-RAY IMAGES WITH ADAPTABLE PARAMETER CONTROL

Paolo Irrera[*][†]   *Isabelle Bloch*[*]   *Maurice Delplanque*[†]

[*]Institut Mines Telecom, Telecom ParisTech, CNRS LTCI, Paris, France - name@telecom-paristech.fr
[†]EOS imaging, Paris, France - mdelplanque@eos-imaging.com

ABSTRACT

A denoising method is proposed for full body X-ray images, acquired under low dose conditions. The suggested algorithm is based on a non local means filter adapted to the statistics of Poisson noise. A new feature of the method is to locally set the filtering parameters in order to denoise while preserving details in low absorption regions. Thus, we propose to adapt the denoising parameters for each pixel by exploiting a global noise level measure and the standard deviation image of the gradient magnitude. Quantitative and visual results on phantom and clinical images show the interest of the method, achieving the objectives.

Index Terms— Low dose X-Ray images, Poisson noise, Non Local Means filter, Adaptive parameters.

1. INTRODUCTION

In this paper we propose a method to reduce the amount of noise present in full body X-ray medical images, acquired under low dose conditions. The statistical model of the noise is a mixture of Gaussian and Poisson distributions. However, when the number of photons collected by the sensor is low, the quantum component is predominant [1]. This occurs typically for acquisitions performed on obese patients or, more generally, for low-dose image acquisitions.

The method is applied to EOS images. EOS imaging is a French company based in Paris that uses Charpak's high energy particle detector to enable low dose X-ray acquisitions [2]. A full body image with no vertical distortion can be obtained through linear vertical scan of the detector in just one acquisition and without the need of stitching algorithms. The main application field of interest is orthopedics. Benchmark studies have shown that EOS system reduces the entrance dose for the patient compared to traditional digital radiography systems (CR, DR) with significant better image quality [3]. Nevertheless, increased patient thickness or decreasing dose increase the level of noise in the images. This is why we propose a method to denoise the images before applying other post-processing algorithms, such as enhancement in low contrast regions. Obviously the denoising process should avoid suppressing useful information, and a robust denoising technique has then to be chosen, with parameters adapted to our context.

Several Poisson denoising algorithms are based on the *Anscombe* variance-stabilizing transform (VST). This operation allows associating the original data with a Gaussian statistical model. It has been formulated by Anscombe in [4] and later generalized by Murtagh et al. in [5] to adapt it to contexts where Gaussian and Poisson noises are mixed up. The final goal of this kind of method is to be able to exploit

well known Gaussian denoising methods. An example is given in [6] where multi-scale image representation is combined with the VST. The main drawback lies in the non-linear distortion of noise-free elements introduced by the transformation. Besides, a more fundamental limit is the non-existence of a perfect variance stabilizing transform for some distributions, like for example the Poisson one [7]. For this reason the VST step should be avoided in our context. Luiser et al. proposed in [8] a wavelets-based method to denoise elements affected by Poisson noise, based on a powerful data-driven technique that exploits an unbiased estimate of the mean square error, called Poisson Unbiased Risk Estimate (PURE). This work was then improved in [1] generalizing to the case of Poisson random vector corrupted by Gaussian noise. Another approach, directly processing the original data set elements, was proposed by Deledalle et al. in [7] and [9]. The main difference is that this approach is based on Non-Local (NL) means, a nonlinear spatial filter that is gaining an increasing popularity in medical image processing for its performance [10]. The idea of handling directly the Poisson noise is a topical subject in image processing as shown in some recent works (e.g. [11]).

In this paper, we propose a denoising method based on Poisson NL means filter convenient to process EOS images and, theoretically, any full body X-Ray image. The objective is to denoise the image while preserving details in low absorption regions, i.e. slightly affected by noise. In particular, the problem of preserving the bone textures while reducing the global amount of noise is addressed in this paper. This goal is achieved by designing an adaptive local setting of parameters, as an original feature of the proposed approach.

The method is part of a larger project which focuses on the design of specific algorithms for low dose X-Ray images. The dose is a central matter in nowadays society as shown by an important medical literature on exposure and related risks of cancer, see for example [12] and [13]. EOS imaging answers the demand of low dose acquisition thanks to its unique system, but at the same time image processing needs to be exploited in order to provide the best image quality and enable specific applications.

The way the method is adapted to our domain of interest is presented in Section 2. In Section 3 results on phantom and real images are provided, along with visual and quantitative evaluations. Conclusions and future developments are outlined in Section 4.

2. POISSON NL-MEANS WITH ADAPTIVE PARAMETER CONTROL

2.1. Poisson NL means

The key idea of NL means is that local is not always synonym of similar. In this type of filter, the pixel values are combined according

to an affinity or similarity measure and not to a simple neighborhood constraint. Thus, in a window Ω centered at any pixel x_i, weights $w_{i,j}$ are defined for each pixel x_j in Ω. Then, the denoised value $\hat{\lambda}_i$ of pixel x_i is estimated using the following weighted mean of the noisy pixel values $k(x_j)$:

$$\hat{\lambda}_i = \frac{\sum_{j=1}^{|\Omega|} w_{i,j} k(x_j)}{\sum_{j=1}^{|\Omega|} w_{i,j}} \qquad (1)$$

For robustness reasons [9], the weight w_{ij} is based on a pixel similarity assessed between patches Ψ around the pixels x_i and x_j, and should be defined according to a suitable statistical model. Given two observations of a Poisson process, k_1 and k_2, two hypotheses are considered: either they share the same underlying noise-free value, i.e. $\lambda_1 = \lambda = \lambda_2$, or they do not, i.e. $\lambda_1 \neq \lambda_2$. Thus, in the case of a Poisson distribution, the similarity function evaluates the likelihood ratio [14] corresponding to the two previous hypotheses [9]:

$$f(k_1, k_2) = -\log\left(\frac{\max_\lambda p(k_1|\lambda_1 = \lambda)p(k_2|\lambda_2 = \lambda)}{\max_\lambda p(k_1|\lambda_1 = \lambda)\max_\lambda p(k_2|\lambda_2 = \lambda)}\right)$$
$$= k_1 \log k_1 + k_2 \log k_2 - (k_1 + k_2)\log\left(\frac{k_1 + k_2}{2}\right) \qquad (2)$$

Note that this formula replaces the Euclidean distance used for Gaussian distributions. Finally, the similarity function in Equation 2 is the input of an exponential kernel of bandwidth α in order to obtain the weights $w_{i,j} \in [0,1]$:

$$w_{i,j} = \exp\left(-\frac{\sum_{x'_i \in \Psi_i}\sum_{x_{j'} \in \Psi_j} f(k(x_{i'}), k(x_{j'}))}{\alpha}\right) \qquad (3)$$

where Ψ_i (respectively Ψ_j) denotes the patch centered at x_i (respectively x_j).

2.2. Alpha Map

It has been shown that in the case of images with a low signal to noise ratio, the quality of the denoising can be improved using a smoothed version of the input [15]. Hence in [9] Equation 3 is redefined using a pre-estimate of the noise-free image and includes an additional similarity term computed between the smoothed image values. This requires an additional filter parameter β, analogous to α. The main aspect of the method proposed in [9] is to set jointly the parameters that control the shape of the exponential, i.e. α and β.

The proposed method differs from Deledalle's one [9] in two main aspects: (i) the smoothed version of the original image is not taken into account, and (ii) we create a map of local alpha values rather than exploiting a global value. For the first aspect, considering that the SNR changes significantly in different zones of the images according to the X-Ray absorption, even if the pre-estimate may globally reduce the noise, in some regions the outcomes could be blurry. A few tests confirmed this idea, thus motivating our decision. As for the second aspect, in medical images it is not trivial to define a global denoising parameter like a threshold or α in our case. Indeed, without prior models, extremely localized structures could fade away along with noise in the filtering processing. Alike, these structures could be saved but with a disappointing effect in other noisy regions. The interest of locally adapted processing has been also highlighted in different contexts. For instance, in [16] Charnigo et al. proposed a semi-local paradigm for wavelet denoising of PET images exploiting a division of the image into suitable blocks that are, then, individually denoised.

Here we want to define a matrix of values of alpha, i.e. *the alpha map*. We propose to exploit measures computed from the standard deviation image of the amplitude of the gradient (from here on referred to as *std image* σ). The alpha map is defined as follows:

$$\alpha(x_i) = M(\eta \zeta(\sigma(x_i))) \qquad (4)$$

where M is an average filter, η is the noise level that gives a hint on the amount of noise present in the image, and $\zeta(.)$ is a curve function of the *std image* value at pixel coordinates x_i. The noise level η is computed as the maximum position of the histogram of the *std image*. This is, basically, the standard deviation computed on the background and provides an indication on the global amount of noise. Thus, for a given image, η is a constant value that modulates $\zeta(.)$. This curve is composed of two growing branches that are interpolated using B-splines to guarantee $\mathbb{C}^1$-regularity. The first part is convex and grows slower than the second one which is concave (see Figure 1). The shape of $\zeta(.)$ is controlled by four parameters. Three parameters define the initial, final and *switch* amplitudes. The fourth parameter is a percentage of the global energy of the *std image* computed on its histogram. This allows defining the end of the first branch. The shape of the ζ curve allows controlling the strength of denoising on the image. The first branch points to regions that correspond to the background and low absorption parts of the body. In this way, the structured details are preserved thanks to a low value of α that practically limits the action of the NL-means filter. Then in the second branch, α grows up quickly to exploit the Poisson NL-means and, thus, to provide accurate denoising. The alpha map is then post-processed via an average
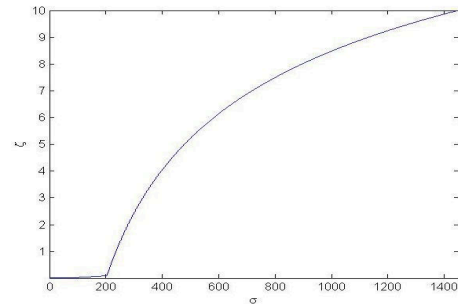

Fig. 1: ζ curve, as a function of the *std image* values. Initial value = 0.01; shift value = 0.1; final value = 10; shift position = 30%.

filter in order to avoid strong transitions and visible changes of spatial resolution in the output image. An example of alpha map, computed on the image displayed in Figure 2(a), is presented in Figure 2(b). For instance, this case shows clearly how our non-linear mapping of α performs well on a clinical image: low values (*cold colors*) correspond mainly to background and bone textures, while the highest values (*hot colors*) are on the pelvis that is a not very much structured zone affected by a significant amount of noise. Finally, we are able to integrate in the classic definition of the Poisson NL means filter (Equation 3) a physical information that is crucial to process diagnostic radiography images, i.e. the absorption of the X-Rays by the patient, which is empirically related to our definition of α. Thanks to this, we solve the problem of poor performance of global methods on textured images already highlighted by Luiser et al. in [8]. The output of the denoising algorithm may still be poor in details, so we have to enhance the contrast. We use in this case a proprietary algorithm based on decomposition in Laplace multiscales. Although denoising and contrast enhancement are antagonist processing steps, what we
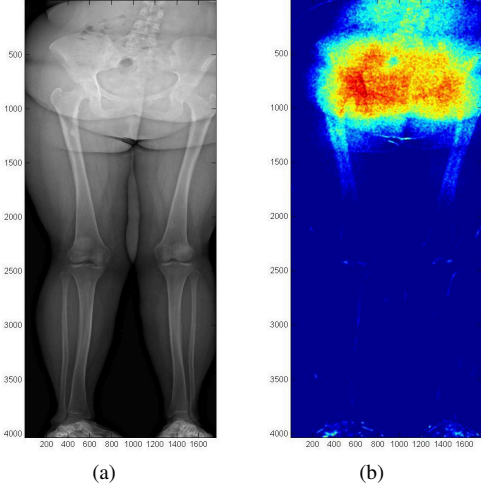
Fig. 2: (a) Input image. (b) Alpha Map: *cold colors* → low α values to preserve the details, *hot colors* → strong α values to reduce noise.

propose here is useful and relevant. Indeed, the contrast enhancement algorithm will benefit of a proper representation of the input image.

3. EXPERIMENTAL RESULTS

The main goal of this section is to evaluate the interest and usefulness of a denoising step before the contrast enhancement. Thus, we will compare the results obtained in a reconstruction pipeline [1] without any denoising, and results obtained with the proposed technique. The contrast enhancement step is the same in both cases. Two types of images are considered for our tests: a phantom (*standard PHD5000 fluoro phantom*) used for image quality evaluations (Figure 3) and patient images (as the one in Figure 2(a)). Besides, for the diagnostic case analyzed in detail, we compared our method with the PURE-LET denoising [8] and Poisson NL-means with global denoising parameters [9]. Note that for the tests conducted here with the global Poisson NL-means, the pre-estimate noise free image used in [9] is neglected, according to the discussion in Section 2.2, and we set $\alpha = \eta$. The standard PHD5000 phantom is covered by a layer of
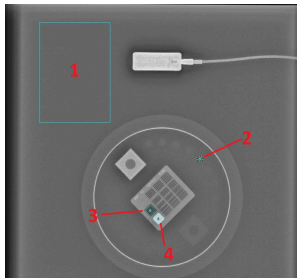

Fig. 3: Standard PHD5000 phantom and regions used for assessing the image quality.

20cm of PMMA blocks in order to simulate the thickness of an adult human body. The peak kilo voltage of the X-Ray generator is fixed at 63 kV. Two parameters can be tuned: the X-Ray tube current and the

exposure time. For five different settings of these parameters, the corresponding dose values were computed: 31.68 μG, 63.48 μG, 97.98 μG, 136.34 μG, and 306.35 μG. As for the denoising parameters, the window size is fixed to 5×7 and the patch size to 3×3. The shape of the $\zeta(.)$ curve, i.e. the alpha map (see Equation 4), is defined according to the acquisition parameters: at lower dose amounts, the noise is more important and a stronger denoising is necessary.

Three quantitative measures are considered: Signal to Noise Ratio (SNR), Contrast to Noise Ratio (CNR) and Dynamic (DYN). The SNR is computed as the ratio of the mean intensity value in a supposedly constant region on its standard deviation (Figure 3 - zone 1). The CNR is estimated in the fifth grey disk of the phantom (Figure 3 - zone 2). Finally, the DYN is computed as the percentage (on the 65536 possible gray levels) of the difference between the mean intensities of zones 3 and 4 (Figure 3). A comparison between the results obtained using the classical and the proposed methods is reported in Figure 4. Using the proposed approach, the SNR gains a
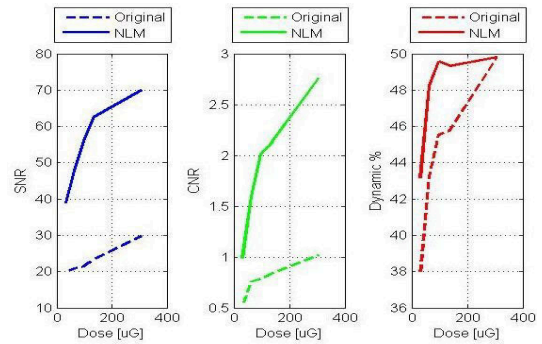

Fig. 4: Image quality metrics on the phantom image: left SNR, center CNR, right DYN. Dotted lines: no specific processing for the noise; continuous lines: proposed NL-means filter with adaptive parameters.

factor two on a linear scale. The dynamics is reduced by 6% between the highest and the lowest dose values rather than 11% using the classical method. The most remarkable improvement concerns the CNR: the disk that is identifiable with the original approach only at 306.35 μG is now visible all along the considered range of doses since the CNR is larger than one.

Let us now illustrate the method on a lower limbs image. We defined two regions of interest (ROI): the head of the femur (Figure 5) and the knee (Figure 6). For instance, the first ROI is important to identify the anterior and posterior acetabulum[2] lips. Instead, the second ROI was chosen in order to verify that the method preserves the bone trabecular structures. The quality of the outputs on the pelvis ROI are quantitatively compared in Table 1. In addition to the SNR (computed in a constant region in the soft tissues) and CNR (computed between two symmetric zones at the borderline of the pelvis bone), to establish whether the loss of resolution is significant or not, we relied on a no reference sharpness measure based on *Local Phase Coherence* (LPC) proposed by Hassen et al. in [17]. This measure is bounded in the interval $[0, 1]$ and we refer to it as IQ_{lpc}. Both the PURE-LET and the global NL-means denoising provide very similar results to those obtained using the classical pipeline, i.e. the global parameters do not allow a sufficiently strong denoising in this ROI. On the contrary, the measures in Table 1 and the picture in Figure 5(b) show a significant improvement of the image quality thanks to the proposed method. The sharpness of the result obtained with the proposed method is reduced but not significantly at all, and the details of

---

[1]Image processing chain that processes the data acquired by the sensor in order to provide a display image that can be clinically interpreted.

[2]Cup-shaped cavity of the pelvis into which the head of the femur fits

Table 1: Pelvis ROI. Quantitative comparison of classical EOS pipeline, PURE-LET [8], global Poisson NL-means [9] and proposed method.

	Classical EOS	PURE-LET [8]	Global NL-means [9]	Proposed
SNR	18.55	19.87	20.52	**21.19**
CNR	1.89	2.14	2.24	**3.08**
IQ_{lpc}	**0.977**	0.976	0.973	0.965

the image are preserved even if the denoising in this ROI is stronger compared to the other two methods. As for the knee region, the re-
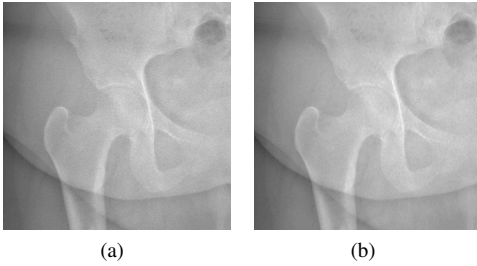

(a)   (b)

Fig. 5: Pelvis ROI of a diagnostic image: (a) Pelvis without denoising, (b) Pelvis after denoising using the proposed method.

sults and the relative sharpness measures are reported in Figure 6. The global Poisson NL-means, in this case, is not good at all because the bone textures fade completely away offering a not realistic outcome. PURE-LET performs better for this ROI, which makes us guess that its global automatic parametrization [8] tends, for our images, to be quite conservative. However, the proposed method is still the best one, according to the IQ_{lpc} value and qualitative comparison. Finally,
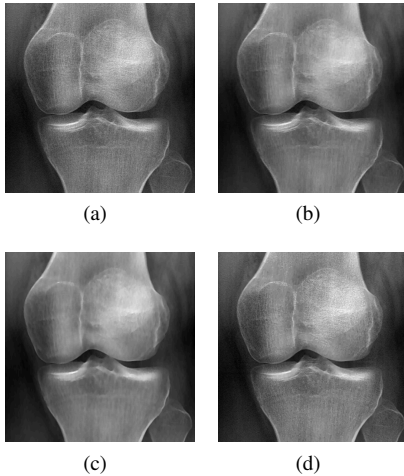

(a)   (b)

(c)   (d)

Fig. 6: Knee ROI of a diagnostic image: (a) Pelvis without denoising $IQ_{lpc} = 0.941$, (b) PURE-LET denoising [8] $IQ_{lpc} = 0.921$, (c) Global Poisson NL-Means [9] $IQ_{lpc} = 0.909$, (d) Proposed method **$IQ_{lpc} = 0.937$**.

we are able to show that our method is suitable to optimally adapt the strength of the denoising to different spots overcoming the drawbacks of other denoising methods. Indeed, the algorithm helps reducing the amount of noise in thick areas, e.g. the pelvis, while preserving the bone details in thinner zones, e.g. the knee. Similar results have been obtained on a series of 20 clinical images.

4. CONCLUSIONS

In this paper, we proposed a new denoising method, by adapting the NL means filter for Poisson noise model introduced in [9] to medical X-Ray images and in particular to those acquired with an EOS system. The main feature of the proposed approach is a local control of the parameters. This allowed us to overcome the drawbacks of other Poisson denoising techniques thanks to the capacity of reducing the amount of noise while preserving the bone textures in low X-rays absorption regions. Quantitative and visual results on both phantom and clinical images have shown the efficiency of the proposed method.

As future work, other potentialities of the technique could be exploited. For example, a contrast enhancement algorithm could be designed in order to reach a better compatibility with the technique introduced in this paper. Anyway, this paper represents a first step towards our main goal: an optimized combination of hardware acquisition system and software processing to improve the image quality of very low dose X-Ray images.

5. REFERENCES

[1] F. Luisier, T. Blu, and M. Unser, "Image Denoising in Mixed Poisson-Gaussian Noise," *IEEE Transactions on Image Processing*, vol. 20, no. 3, pp. 696–708, March 2011.

[2] J. Dubousset, G. Charpak, and W. Skalli, "Skeletal and spinal imaging with EOS system," *Archives de Pédiatrie*, vol. 15, no. 5, pp. 665–666, 2008.

[3] S. Deschênes, G. Charron, and G. Beaudoin, "Diagnostic imaging of spinal deformities: reducing patients radiation dose with a new slot-scanning X-ray imager," *The Spine Journal*, vol. 35, no. 9, pp. 989–994, 2010.

[4] F. J. Anscombe, "The transformation of Poisson binomial and negative-binomial data," *Biometrika*, vol. 35, no. 3, pp. 246–254, December 1948.

[5] F. Murtagh, J.-L. Starck, and A. Bijaoui, "Image restoration with noise suppression using a multiresolution support," *Astron. Astrophys Supplement Series*, vol. 112, pp. 179–189, 1995.

[6] B. Zhang, J. M. Fadili, and J.-L. Starck, "Wavelets, ridgelets, and curvelets for Poisson noise removal," *IEEE Transactions on Image Processing*, vol. 17, no. 7, pp. 1093–1108, July 2008.

[7] C.-A. Deledalle, L. Denis, and F. Tupin, "How to compare noisy patches? Patch similarity beyond Gaussian noise," *International Journal of Computer Vision*, vol. 99, no. 1, pp. 86–102, 2012.

[8] F. Luisier, C. Vonesch, T. Blu, and M. Unser, "Fast Interscale Wavelet Denoising of Poisson-Corrupted Images," *Signal Processing*, vol. 90, no. 2, pp. 415–427, February 2010.

[9] C.-A. Deledalle, F. Tupin, and L. Denis, "Poisson NL Means: Unsupervised Non Local Means for Poisson Noise," in *IEEE International Conference on Image Processing (ICIP)*, Hong Kong, China, September 2010, pp. 801–804.

[10] A.T. Vega, V.G. Perez, S.A. Fernandez, and C.F. Westin, "Efficient and robust nonlocal means denoising of MR data based on salient feature matching," *Computer Methods and Programs in Biomedicine*, vol. 105, no. 2, pp. 131–144, February 2012.

[11] J. Salmon, C-A. Deledalle, R. Willett, and Z. T. Harmany, "Poisson Noise Reduction with Non-Local PCA," in *IEEE International Conference on Acoustics, Speech and Signal Processing (ICASSP12)*, March 2012, pp. 1109 – 1112.

[12] M.M. Ronckers, C.M. et Doody, J.E. Lonstein, M. Stovall, and Land C.E., "Multiple diagnostic X-rays for spine deformities and risk of breast cancer," *Cancer Epidemiol Biomarkers Prev*, vol. 17, no. 3, pp. 605–613, March 2008.

[13] R. Smith-Blindman, Miglioretti D.L., and Johnson E., "Use of Diagnostic Imaging Studies and Associated Radiation Exposure for Patients Enrolled in Large Integrated Health Care Systems, 1996-2010," *The Journal of American Medical Association*, vol. 307, no. 22, pp. 2400–2409, June 2012.

[14] S. Kay, *Fundamentals of statistical signal processing*, vol. 2, Prentice Hall, 1998.

[15] C. Kervrann and J. Boulanger, "Optimal spatial adaptation for patch-based image denoising," *IEEE Transactions on Image Processing*, vol. 15, no. 10, pp. 2866–2878, 2007.

[16] R. Charnigo, J. Sun, and R.J. Muzic, "A Semi-Local Paradigm for Wavelet Denoising," *IEEE Transactions on Image Processing*, vol. 15, no. 3, pp. 666–677, March 2006.

[17] R. Hassen, Z. Wang, and M. Salama, "No-Reference Image Sharpness Assessment Based on Local Phase Coherence Measurement," in *IEEE International Conference on Acoustics, Speech and Signal Processing (ICASSP10)*, March 2010, pp. 2434 – 2437.